

PROCEEDINGS OF SPIE

[SPIDigitalLibrary.org/conference-proceedings-of-spie](https://spiedigitallibrary.org/conference-proceedings-of-spie)

Mid-IR high-index dielectric Huygens metasurfaces

Jun Ding, Li Zhang, Han Ren, Mi Zhou, Yuankun Lin, et al.

SPIE.

Mid-IR High-index Dielectric Huygens' Metasurfaces

Jun Ding¹, Li Zhang^{2,3}, Han Ren⁴, Mi Zhou⁴,
Yuankun Lin^{4,5}, Juejun Hu², and Hualiang Zhang^{1*}

¹ECE Department, University of Massachusetts Lowell

²MSE Department, Massachusetts Institute of Technology

³National Engineering Research Center of Electromagnetic Radiation Control Materials,
University of Electronic Science and Technology of China

⁴EE Department, University of North Texas

⁵Physics Department, University of North Texas

ABSTRACT

In this paper, we proposed highly efficient all-dielectric Huygens' metasurfaces working at mid-IR frequencies. The meta-atom of the designed Huygens' metasurface is a cubic dielectric resonator or its variety, which is made from PbTe that possesses a high refractive index of around 5 at mid-IR frequencies. By overlapping spectrally both the magnetic and electric dipole modes of the high-index dielectric resonators, a full phase coverage of 2π and an equal-magnitude transmission could be achieved, which are essential conditions for realizing a metasurface. Two Huygens' metasurfaces for beam bending are designed with a phase change between two consecutive meta-atoms of $\pi/4$ and $\pi/3$, respectively. The simulation results agree well with the design theory.

Keywords: Huygens' metasurface, high-index material, mid-IR, dielectric resonators

1. INTRODUCTION

Metasurfaces^{1,2} are planar 2D structures with subwavelength thicknesses, allowing complete control of the phase, amplitude, and/or the polarization of the incident light. Compared to conventional bulky optical devices, which rely on the phase accumulation along the long propagation distances, metasurfaces facilitate strong light-matter interaction with subwavelength resonant elements, which allow us to tailor the phase profile across the thin interfaces. In the early stage of the development of metasurfaces, metallic resonators (i.e., antennas) and/or their counterparts (i.e., slot antennas)³⁻⁷ were usually adopted as the building block to realize a number of fascinating functionalities, e.g., anomalous reflection and refraction, holography, flat lens. However, the use of metallic resonators exhibits high intrinsic ohmic losses at infrared and higher frequencies, which hinders their use in metamaterials based on resonance. In order to satisfy 2π phase coverage and near equal transmission, which are required by a metasurface, the cross-polarized component of the incident light is utilized, which further reduces the efficiency of the metasurface. For instance, the cross-polarized transmission amplitudes for the C-shape and V-shape resonators are typically less than 0.4 and 0.15^{3,6,7}, respectively. Much research effort has been devoted to improve the efficiency of the metasurface by using reflection type structures⁸⁻¹¹ or multilayer structures¹²⁻¹⁵. Recently, experimental demonstrations of a new type of multilayer metasurface called Huygens' surfaces at microwave frequencies and telecommunication wavelengths have been presented¹⁶⁻¹⁸, in which the crossed magnetic and electric dipoles (Huygens' source) can both be induced by the multi metallic layers. Although the efficiency is improved, the Huygens' surfaces based on these metallic layers still suffer from large ohmic loss. It is reported that high-index dielectric resonators (DRs) can naturally support both magnetic and electric resonances¹⁹, which represent a promising alternative for the development of high-efficiency Huygens' surfaces because they replace lossy ohmic currents with low-loss displacement currents. Thus, high-efficiency dielectric Huygens' surfaces have been studied and experimentally demonstrated at telecommunication wavelengths based on silicon.

*hualiang_zhang@uml.edu; phone: 940-595-7220; fax: 978-934-3027

all-dielectric Huygens' metasurfaces based on the transparent material PbTe working at mid-IR frequencies are demonstrated, which avoid the conduction loss compared to the plasmonic counterparts. PbTe is employed to construct the proposed metasurfaces, providing a high refractive index of around 5 at mid-IR frequencies. By tailoring the aspect ratio of the height and length of the DRs, the magnetic and electric dipole modes of the DRs can be manipulated to overlap spectrally, resulting in a full phase control of 2π and a near-unity transmission, which are essential requirements for a high-efficiency metasurface. Thus, the high-index DRs could be deemed as Huygens' sources and can be used as the meta-atom of a metasurface. The meta-atom of the proposed Huygens' metasurface is a cubic DR or its derivatives by perturbing the shape of the cuboid in order to shift the DR's overlapping resonances at identical aspect ratios. Two Huygens' metasurfaces for bending the incident waves are designed with a phase interval between two consecutive meta-atoms of $\pi/4$ and $\pi/3$, respectively. The proposed design concept is verified by the simulation results. The proposed all-dielectric Huygens' metasurfaces can find numerous applications in optical devices, including beam-forming, beam-steering, holography and dispersion control.

2. DESIGN OF THE PROPOSED STRUCTURES

Figure 1(a) schematically depicts a unit cell of the DR, which is a PbTe cubic backed by a substrate of Calcium fluoride (CaF₂). In our interested frequency range 55~59 THz, the PbTe has a high refractive index around 5 with almost negligible loss²⁰, and the CaF₂ substrate is modeled as a lossless, infinite half space with refractive index of 1.396. As shown in Figure 1(a), the height of the cubic DR or its derivatives (e.g., H-shape in Figure 1(b)) is fixed at $H=0.65\mu\text{m}$, and the electric and magnetic resonances can be tuned via varying the geometry of the DRs (i.e., the L_x , L_y , L_{xd} and L_{yd}). The H-shape DR in Figure 1(b) is introduced to achieve the desired resonant properties in order to satisfy the size and spacing requirements in the fabrication according to the perturbation theory²¹. We applied commercial full-wave simulator (CST Microwave Studio) to perform the numerical simulation. In the following simulations, an x-polarized incident wave propagates in Z-direction from the bottom substrate. The periodicity of the unit cell and the dimensions of the DRs are labeled in Figure 1 as P , L_x , L_y , L_{xd} , and L_{yd} . The designed metasurfaces are investigated in the mid-infrared frequency range, which is around 55~59 THz.

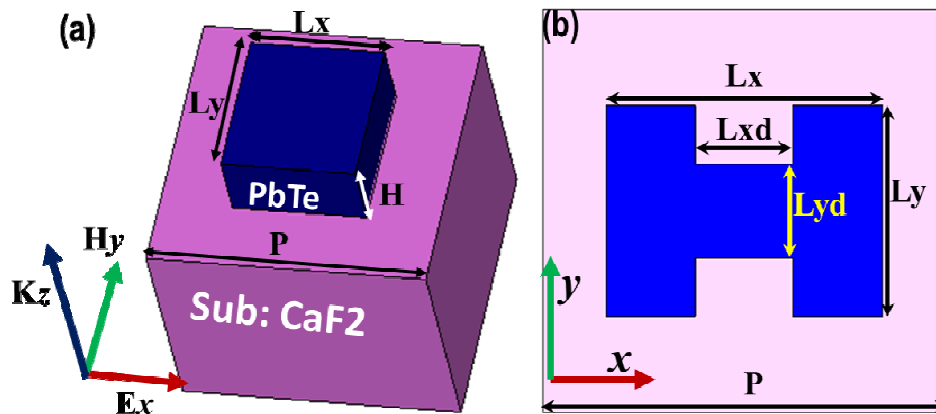


Figure 1: (a) Schematic of a unit cell of the dielectric resonator. (The blue and magenta represent PbTe and CaF₂, respectively.) (b) Schematic of an H-shape DR.

3. RESULTS AND DISCUSSIONS

3.1. Huygens' metasurface with $\pi/4$ phase increment

First, we studied the Huygens' surface with a $\pi/4$ phase increment. The schematic of the 8-DR supercell is shown in the lower part of Figure 2, which plots the phase shift and transmission amplitude for these 8 DRs. The supercell contains 8

meta-atoms with dimensions detailed in Table I, where each meta-atom is responsible for a $\pi/4$ phase discontinuity between two consecutive meta-atoms. The phase shift and the transmission amplitude for the eight meta-atoms are plotted in Figure 2. It can be seen from Figure 2 that the transmission amplitudes are very high (all over 0.91), indicating a highly efficient metasurface. Two H-shape DRs are introduced to increase the spacing between two adjacent meta-atoms in the supercell for the ease of fabrication.

Table I: Dimensions for the Eight Meta-atoms

Cell No. Dimensions	1	2	3	4	5	6	7	8
Lx (Lxd) μm	2.4	2	2 (0.7)	1.8(0.6)	2.1	1.75	1.25	0.55
Ly (Lyd) μm	1.3	1.3	1.9(0.98)	1.9(0.9)	0.9	0.8	0.8	0.7

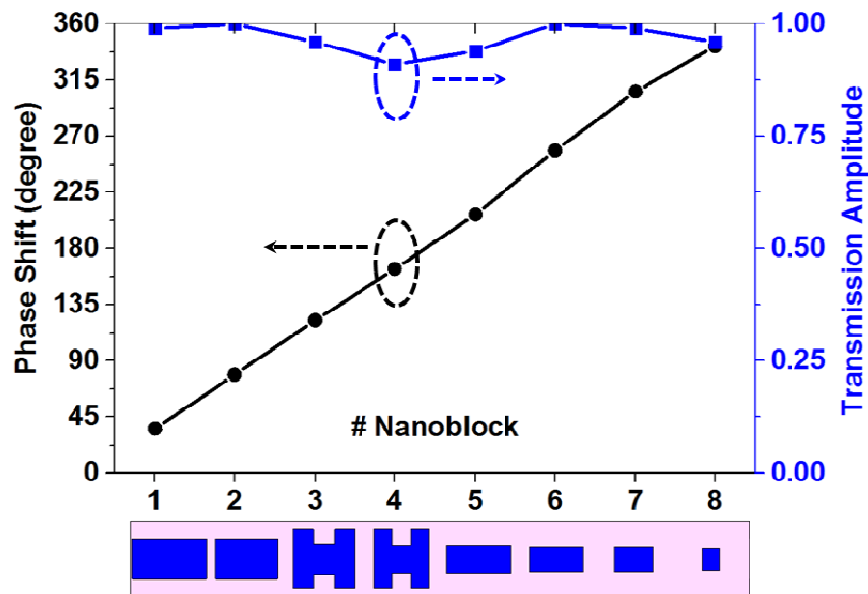


Figure 2. The phase shift and transmission amplitude for each cell in a supercell with 8 nano-blocks. The transmission amplitude is very high (over 0.9). The schematic of the supercell is shown in the lower part.

Figure 3(a) illustrates the normalized far-field transmission spectrum at 57 THz. Notice that there are two strong lobes, one is at around 0 degree, corresponding to the light transmitted in the normal direction ($n=0$ harmonic), the other is at around -13.7° , corresponding to the designed anomalous deflection ($n=-1$ harmonic). As pointed out in¹⁶, $n=-1$ harmonic can be optimized by suppressing $n=0$ harmonic, which cannot be avoided. The anomalous deflection angle can be calculated by the generalized Snell's law³ by

$$\theta_t = \arcsin\left(\frac{\lambda_0}{2\pi} \frac{d\Phi}{dx}\right) = \arcsin\left(\frac{\lambda_0}{2\pi} \frac{2\pi/N}{P}\right) \quad (1)$$

where N is the number of the supercell for 2π phase coverage and P is the periodicity of the unit cell. The theoretically calculated deflection angle is -15.3° at 57 THz, agreeing well with the numerical simulation result -13.7° . Figure 3(b) plots the simulated E-field distribution at 57 THz, where a uniform anomalous transmitted wave is observed.

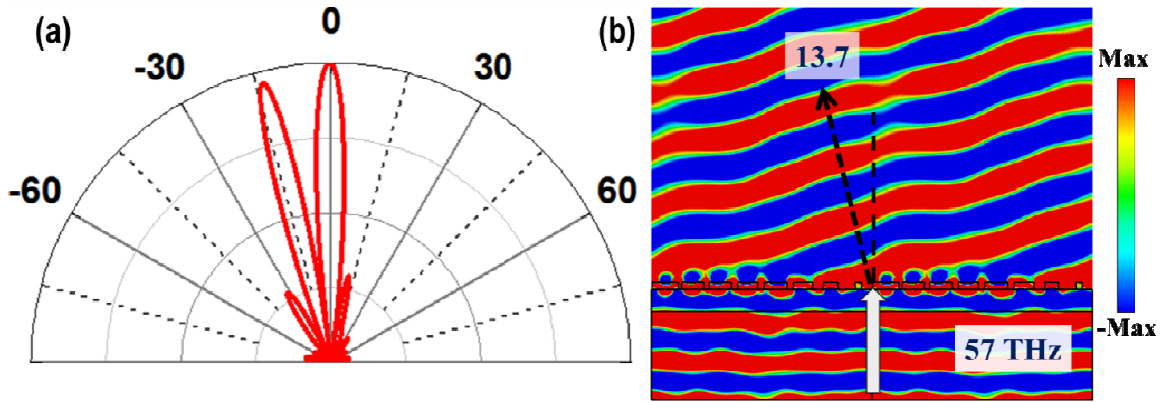


Figure 3. (a) The normalized far-field transmission spectrum at 57 THz. (b) The x-component E-field distribution at 57 THz with an x-polarized incident wave propagating in Z-direction

Table II: Dimensions for the Six Meta-atoms

Cell No. Dimensions	1	2	3	4	5	6
Lx (Lxd) μm	1.75	1.8	1.8(0.6)	2	1.35	0.5
Ly (Lyd) μm	1.35	1.3	1.9(0.9)	0.85	0.85	0.5

3.2. Huygens' metasurface with $\pi/3$ phase increment

Next, we investigate a Huygens' surface with a $\pi/3$ phase increment. The schematic of the 6-DR supercell is shown in the lower part of Figure 4, which plots the phase shift and transmission amplitude for these 6 DRs. Once again, high transmission amplitudes (around 0.9) for all resonators except number 1 (which is 0.86) can be observed. The dimensions for each cell are listed in Table II.

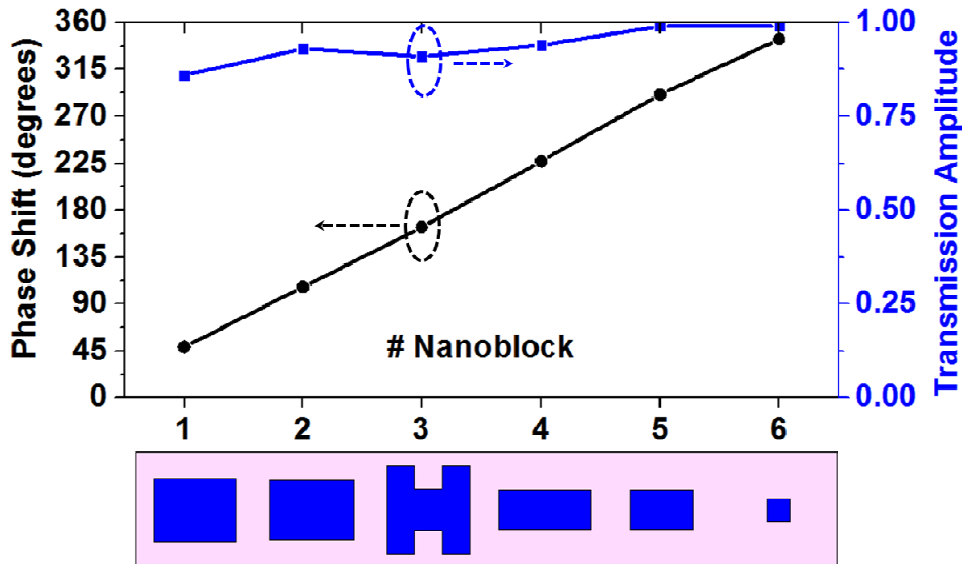


Figure 4. The phase shift and transmission amplitude for each cell in a supercell with 8 nano-blocks. The transmission amplitude is very high (around 0.9, except number 1, which is 0.86). The schematic of the supercell is shown in the lower part.

We plotted the amplitude transmission spectrum as a function of frequency and transmitted angle in Figure 5. We observe two strong straps corresponding to the $n=0$ (at around 0°) and $n=-1$ (at around -20°) harmonics, respectively. We also plotted the theoretical values for the deflection angles at our interested frequency range (i.e., 55~59 THz) in red dash line. The theoretical predictions agree very well with the simulated results. Specifically, the simulated deflection angle at 57 THz is -19.4° , which is very close to the theoretical value of -20.5° .

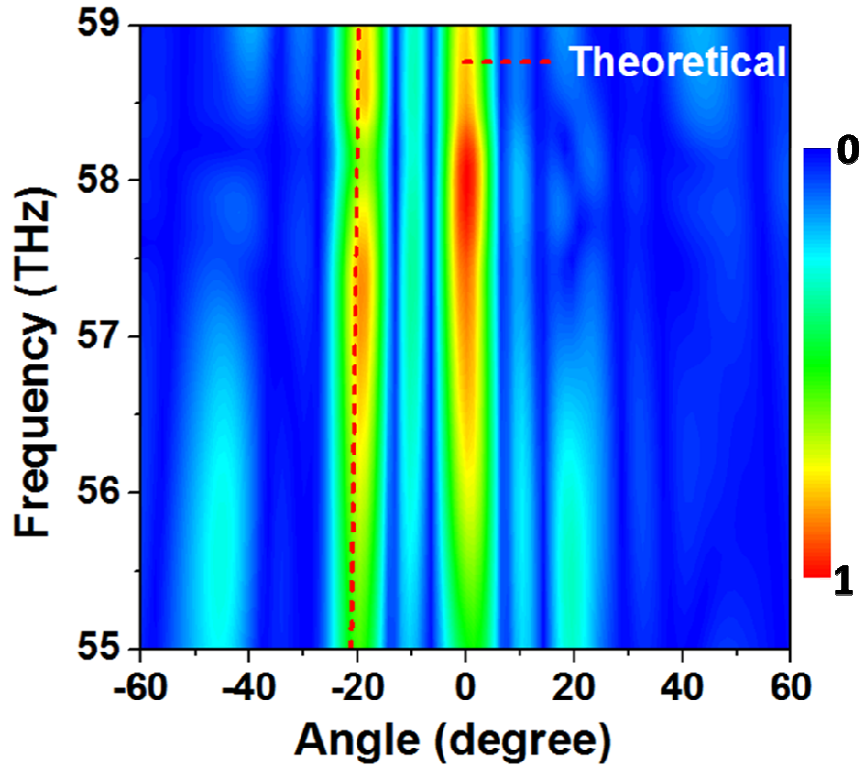


Figure 5. Amplitude transmission spectrum as a function of frequency and transmitted angle.

4. CONCLUSIONS

In this paper, we have used the DRs made from PbTe to construct highly efficient Huygens' metasurfaces at the mid-IR frequency range. Two Huygens' metasurfaces composed of 8-cell and 6-cell supercells are designed and simulated to deflect the incident wave to the anomalous direction at 57 THz. The transmission amplitude for each cell has a large value (around 0.9), indicating a high efficiency. The simulated results agree very well with the theoretical predictions. The proposed all-dielectric Huygens' metasurfaces can be used to achieve a number of functionalities such as beam deflecting, focusing, and holography.

ACKNOWLEDGEMENTS

This work is supported partially by the research grant from the U.S. National Science Foundation under the Grant No. CMMI-1266251,

REFERENCES

- [1] Holloway, C. L., Kuester, E. F., Gordon, J. A., O'Hara, J., Booth, J., Smith, D. R., "An Overview of the Theory and Applications of Metasurfaces: The Two-Dimensional Equivalents of Metamaterials," *IEEE Antennas and Propagation Magazine* **54**(2), 10–35 (2012).
- [2] Yu, N., Capasso, F., "Flat optics with designer metasurfaces," *Nature Materials* **13**(2), 139–150 (2014).
- [3] Yu, N., Genevet, P., Kats, M. A., Aieta, F., Tetienne, J.-P., Capasso, F., Gaburro, Z., "Light Propagation with Phase Discontinuities: Generalized Laws of Reflection and Refraction," *Science* **334**(6054), 333–337 (2011).
- [4] Aieta, F., Genevet, P., Kats, M. A., Yu, N., Blanchard, R., Gaburro, Z., Capasso, F., "Aberration-Free Ultrathin Flat Lenses and Axicons at Telecom Wavelengths Based on Plasmonic Metasurfaces," *Nano Letters* **12**(9), 4932–4936 (2012).
- [5] Ni, X., Kildishev, A. V., Shalaev, V. M., "Metasurface holograms for visible light," *Nature Communications* **4** (2013).
- [6] Zhang, X., Tian, Z., Yue, W., Gu, J., Zhang, S., Han, J., Zhang, W., "Broadband Terahertz Wave Deflection Based on C-shape Complex Metamaterials with Phase Discontinuities," *Adv. Mater.* **25**(33), 4567–4572 (2013).
- [7] Wang, Q., Zhang, X., Xu, Y., Tian, Z., Gu, J., Yue, W., Zhang, S., Han, J., Zhang, W., "A Broadband Metasurface-Based Terahertz Flat-Lens Array," *Advanced Optical Materials* **3**(6), 779–785 (2015).
- [8] Sun, S., Yang, K.-Y., Wang, C.-M., Juan, T.-K., Chen, W. T., Liao, C. Y., He, Q., Xiao, S., Kung, W.-T., et al., "High-Efficiency Broadband Anomalous Reflection by Gradient Meta-Surfaces," *Nano Letters* **12**(12), 6223–6229 (2012).
- [9] Grady, N. K., Heyes, J. E., Chowdhury, D. R., Zeng, Y., Reiten, M. T., Azad, A. K., Taylor, A. J., Dalvit, D. A. R., Chen, H.-T., "Terahertz Metamaterials for Linear Polarization Conversion and Anomalous Refraction," *Science* **340**(6138), 1304–1307 (2013).
- [10] Pors, A., Albrektsen, O., Radko, I. P., Bozhevolnyi, S. I., "Gap plasmon-based metasurfaces for total control of reflected light," *Scientific Reports* **3** (2013).
- [11] Zheng, G., Mühlenbernd, H., Kenney, M., Li, G., Zentgraf, T., Zhang, S., "Metasurface holograms reaching 80% efficiency," *Nature Nanotechnology* **10**(4), 308–312 (2015).
- [12] Wei, Z., Cao, Y., Su, X., Gong, Z., Long, Y., Li, H., "Highly efficient beam steering with a transparent metasurface," *Optics Express* **21**(9), 10739 (2013).
- [13] Yang, Q., Gu, J., Wang, D., Zhang, X., Tian, Z., Ouyang, C., Singh, R., Han, J., Zhang, W., "Efficient flat metasurface lens for terahertz imaging," *Opt. Express* **22**(21), 25931–25939 (2014).
- [14] Pfeiffer, C., Grbic, A., "Metamaterial Huygens' Surfaces: Tailoring Wave Fronts with Reflectionless Sheets," *Phys. Rev. Lett.* **110**(19), 197401 (2013).
- [15] Monticone, F., Estakhri, N. M., Alù, A., "Full Control of Nanoscale Optical Transmission with a Composite Metascreen," *Physical Review Letters* **110**(20) (2013).
- [16] Pfeiffer, C., Emani, N. K., Shaltout, A. M., Boltasseva, A., Shalaev, V. M., Grbic, A., "Efficient Light Bending with Isotropic Metamaterial Huygens' Surfaces," *Nano Letters* **14**(5), 2491–2497 (2014).
- [17] Decker, M., Staude, I., Falkner, M., Dominguez, J., Neshev, D. N., Brener, I., Pertsch, T., Kivshar, Y. S., "High-Efficiency Dielectric Huygens' Surfaces," *Advanced Optical Materials*, n/a – n/a (2015).
- [18] Shalaev, M. I., Sun, J., Tsukernik, A., Pandey, A., Nikolskiy, K., Litchinitser, N. M., "High-Efficiency All-Dielectric Metasurfaces for Ultracompact Beam Manipulation in Transmission Mode," *Nano Letters* **15**(9), 6261–6266 (2015).
- [19] Ginn, J. C., Brener, I., Peters, D. W., Wendt, J. R., Stevens, J. O., Hines, P. F., Basilio, L. I., Warne, L. K., Ihlefeld, J. F., et al., "Realizing Optical Magnetism from Dielectric Metamaterials," *Phys. Rev. Lett.* **108**(9), 097402 (2012).
- [20] Wang, J., Hu, J., Sun, X., Agarwal, A. M., Kimerling, L. C., Lim, D. R., Synowicki, R. A., "Structural, electrical,

and optical properties of thermally evaporated nanocrystalline PbTe films,” *Journal of Applied Physics* **104**(5), 053707 (2008).

- [21] Campione, S., Basilio, L. I., Warne, L. K., Sinclair, M. B., “Tailoring dielectric resonator geometries for directional scattering and Huygens’ metasurfaces,” *Optics Express* **23**(3), 2293 (2015).